HHS Public Access

Author manuscript

*Environ Sci Nano*. Author manuscript; available in PMC 2018 November 01.

Published in final edited form as:

*Environ Sci Nano*. 2017 November 1; 4(11): 2144–2156. doi:10.1039/C7EN00573C.

# Synergistic effects of engineered nanoparticles and organics released from laser printers using nano-enabled toners: potential health implications from exposures to the emitted organic aerosol

**Marie-Cecile G. Chalbot**[a,*], **Sandra V. Pirela**[b,*], **Laura Schifman**[c], **Varun Kasaraneni**[c], **Vinka Oyanedel-Craver**[c], **Dhimiter Bello**[b], **Vincent Castranova**[d], **Yong Qian**[e], **Treye Thomas**[f], **Ilias G. Kavouras**[a], and **Philip Demokritou**[b]

[a]Department of Environmental Health Sciences, University of Alabama at Birmingham, Birmingham, Alabama [b]Department of Environmental Health, Center for Nanotechnology and Nanotoxicology, T.H. Chan School of Public Health, Harvard University, Boston, Massachusetts [c]Department of Civil and Environmental Engineering, University of Rhode Island, Kingston, Rhode Island [d]Department of Pharmaceutical Sciences/School of Pharmacy, West Virginia University, Morgantown, West Virginia [e]Pathology and Physiology Research Branch, Health Effects Laboratory Division, National Institute for Occupational Safety and Health, Morgantown, West Virginia [f]U.S. Consumer Product Safety Commission, Office of Hazard Identification and Reduction, Rockville, Maryland

## Abstract

Recent studies have shown that engineered nanoparticles (ENPs) are incorporated into toner powder used in printing equipment and released during their use. Thus, understanding the functional and structural composition and potential synergistic effects of this complex aerosol and released gaseous co-pollutants is critical in assessing their potential toxicological implications and risks. In this study, toner powder and PEPs were thoroughly examined for functional and molecular composition of the organic fraction and the concentration profile of 16 Environmental Protection Agency (EPA)-priority polycyclic aromatic hydrocarbons (PAH) using state of the art analytical methods. Results show significant differences in abundance of non-exchangeable organic hydrogen of toner powder and PEPs, with a stronger aromatic spectral signature in PEPs. Changes in structural composition of PEPs are indicative of radical additions and free-radical polymerization favored by catalytic reactions, resulting in formation of functionalized organic species. Particularly, accumulation of aromatic carbons with strong styrene-like molecular signatures on PEPs is associated with formation of semivolatile heavier aromatic species (*i.e.*,

Correspondence to: Ilias G. Kavouras; Philip Demokritou.

*Equally contributing first authors.

Electronic Supplementary Information (ESI) available: [details of any supplementary Information available should be included here]. See DOI: 10.1039/x0xx00000x

**Disclaimer**

The findings and conclusions in this report are those of the authors and do not necessarily represent views of the National Institute for Occupational Safety and Health or the Consumer Protection Safety Commission.

PAHs). Further, the transformation of low molecular weight PAHs in the toner powder to high molecular weight PAHs in PEPs was documented and quantified. This may be a result of synergistic effects from catalytic metal/metal oxide ENPs incorporated into the toner and the presence/release of semi-volatile organic species (SVOCs). The presence of known carcinogenic PAHs on PEPs raises public health concerns and warrants further toxicological assessment.

## Introduction

It has been established that toner-based printing equipment, such as laser printers and photocopiers, release particles in the ultrafine/nano size range ($PM_{0.1}$, particulate matter with aerodynamic diameter less than 100 nm) (1–4). More recently, it was established that the toners used in printing equipment, such as laser printers and photocopiers, have become nano–enabled products (NEPs) since various engineered nanoparticles (ENPs) were added to their formulation in order to enhance printing quality. Such nanoscale additives include iron, titanium, silicon, copper, manganese, sulfur, aluminum, tin, zinc, and manganese, mostly as oxides (1,2,5). Further, it was previously concluded by our group, that such ENPs are released and become airborne during use (printing) (1,6,7).

It has been shown that ENPs due to their nanoscale size may penetrate into the deepest regions of the lungs and settle in the alveoli; thus, potentially translocating into the blood stream to induce harmful effects (8–13). For example, intratracheal instillation of silica-coated zinc oxide led to a significant dose-response inflammatory response evident by an increased presence of neutrophils and myeloperoxidase, lactate dehydrogenase and albumin in the bronchoalveolar lavage fluid of the exposed rats (12).

A number of studies have focused on the exposure characterization of emissions from laser printers (14). Early on, it was documented that an increase in particle number concentrations of up to $3.8\times10^4$ particles/$cm^3$ with a count median diameter varying from 40–76 nm in an office during printing, which suggests the majority of measured particles have sizes less than 100 nm ($PM_{0.1}$) (15–17). Other studies (4)Schripp, Wensing [1]Schripp, Wensing [1]Schripp, Wensing [1] also reported $PM_{0.1}$ was emitted from laser printers at concentrations of $1.1\times10^5$ to $2.2\times10^6$ particles/$cm^3$ with aerodynamic diameters in the range of 22–40 nm. In addition to laser printers, a recent industry wide exposure assessment of 15 photocopy centers in Massachusetts; confirmed high particle concentrations from $1.9\times10^3$ to $2.3\times10^4$ particles/$cm^3$ and reached levels as high as $2.17\times10^5$ particles/$cm^3$ (6). Previous publications have documented high levels of $PM_{0.1}$ concentrations over $1.4\times10^6$ particles/$cm^3$, which were up to 12 times higher than the background levels (7).

More recently, our group has developed a Printer Exposure Generation System (PEGS) to systematically generate and sample airborne PEPs (2). The PEGS was used to perform a thorough physicochemical and morphological assessment of PEPs for eleven widely used laser printers. The study concluded that laser printers currently in the market could emit over $10^6$ particles/$cm^3$. Moreover, the PM released had mean particle diameters ranging from 39 to 138 nm (2). More importantly, it has been confirmed that several ENPs were incorporated into toner formulations (*e.g.*, silica, alumina, titania, ceria, iron oxide, zinc oxide, copper oxide, and carbon black, among others) and released into the air during printing. The

analyzed toner powders contained large amounts of organic carbon (OC, 42–89%), metals/metal oxides (1–33%), and elemental carbon (EC, 0.33–12%). Similarly, the PEPs had a chemical composition comparable to that of the toner, which contained 50–90% OC, 0.001–0.5% EC and 1–3% metals. While the chemistry of the PEPs generally reflected that of their toners, considerable differences were documented, which are indicative of potential transformations taking place during consumer use (printing). However, the organic speciation of PEPs and formation mechanisms remained unknown.

As far as the evaluation of potential toxicity of the PEPs, evidence continues to grow in the published domain as summarized in a review paper (14) and includes both *in vitro* and *in vivo* toxicological studies as well as human health studies. In our previous studies, it was found that human small airway epithelial cells, microvascular endothelial cells, macrophages, and lymphoblasts showed substantial changes in cell viability, production of reactive oxygen species, release of inflammatory cytokines and modifications to the DNA methylation machinery (18–20). Animal experimental models have also confirmed the findings stated previously, including upregulation of neutrophils, macrophages and changes in the expression of genes that are involved in both the repair process from oxidative damage and the initiation of immune responses to foreign pathogens (21,22). Various epidemiological studies with detailed exposure characterization data have been done in photocopy centers. Specifically, one group (23) observed a significant increase in inflammatory and oxidative DNA damage indicators in individuals exposed to emissions from photocopiers. Elango and colleagues (24) performed a more detailed assessment in copier operators in India and discovered that the workers were experiencing higher prevalence of nasal blockage, cough, excessive sputum production, and breathing difficulties in addition to elevated markers for oxidative stress and lower albumin to globin ratio, among other important health parameters. Other investigators evaluating the health of photocopier operators in various countries have identified similar findings as those previously mentioned (25–27).

Here, emphasis was given to the *in situ* functional and molecular composition of the PEPs-associated organic fraction and its relationship to precursor organic compounds in toner powder. By using nuclear magnetic resonance (NMR) spectroscopy, we identified the abundant functional groups and species in PEPs and toner powder to determine which organic species are present in PEPs. Further, we aimed to understand whether compounds formed during the printing process are enriched in PEPs due to interactions of gaseous and ENP byproducts of the printing process. NMR spectroscopy allows for the characterization of ultra-complex and multiphase samples as a whole in a non-destructive, repeatable and consistent manner. In addition to NMR analysis, specific attention has been paid to polycyclic aromatic hydrocarbons (PAHs), which can be formed due to the elevated operating temperatures during the printing process (*e.g.*, approximately 200°C) and potential synergistic interactions due to the presence of catalytic ENPs, which may result in formation of highly mutagenic oxygenated and nitrated polycyclic aromatic compounds (28). We hypothesize that the release of low molecular weight gaseous PAHs (LMPAHs) from toner powders and co-existence with nanoscale catalytic ENPs added in the toners (*i.e.*, Fe, Al, Cu, Ti, among others) can enrich the high molecular weight PAHs (HMPAHs) of PEPs and increase their carcinogenic potential; thus, creating a nano-specific mechanism of deposition

of such toxins in the lung. This is a critical knowledge gap and a detailed chemical speciation of PEPs is needed in order to identify mechanistic pathways and potential adverse health effects.

## Experimental

### Generation and collection of size-fractionated PEPs and toner powder

The exposure platform (PEGS) recently developed by our group was used for the generation of the exposures and sampling of PEPs. Detailed descriptions of the PEPs generation, collection and extraction methods used have been published elsewhere (2,5)[2][2][2]. Briefly, a high emitting laser printer (identified as B1 in previously published studies) was placed inside an environmental chamber and set to print single-sided monochrome documents with a 5%-page coverage. PEPs were collected during the use of the laser printer and separated into different size fractions ($PM_{0.1}$ and $PM_{2.5}$) on polyurethane foam substrates (PUF) and Teflon filters using the Harvard Compact Cascade Impactor, which operated at 30 l/min according to the nominal equivalent cutoff diameters at 50% efficiency (52)[3][3][3]. The PUF substrates and filters were weighed pre- and post-sampling following a 48-hour stabilization process in a temperature- (22°C ± 1) and humidity- (43% ± 2) controlled environmental chamber utilizing a Mettler Toledo XPE analytical microbalance. After sampling the size-fractionated PEPs, the particles were extracted from the collection filter into deionized water (DI $H_2O$) using an aqueous suspension methodology (5,53,54). Toner powder was also retrieved from laser printer toner cartridges and transferred to clean scintillation vials for subsequent chemical analysis.

### NMR Spectroscopy

The collection media were ultrasonically extracted with 2 ml of ultrapure $H_2O$, lyophilized using a Speed-Vac system, and transferred with 400 μl of $H_2O$ to 5.0 mm Norell NMR tubes for analysis. An aliquot of 200 μl of a $HPO_4^{2-}/H_2PO_4^-$ (pH 7.4), (trimethylsilyl)propionic acid-$d_4$ (TSP-$d_4$ 1mM) and $NaN_3$ (3mM) solution in $D_2O/H_2O$ (30/70 v/v) was added. NMR spectra were acquired at 300 K using a Bruker Avance III spectrometer operating at 600.17 MHz with a protonoptimized triple resonance “inverse” 5-mm cryogenic probe CP TCI600S3 H-C/N-D-05 Z fitted with an actively-shielded single axis z-gradient, and digital quadrature detection (DQD, 10 μs prescan delay) using TopSpin 3.5/PL6 software (Bruker BioSpin Corp., Billerica, MA).

### 1D $^1$H and 2D $^1$H-$^1$H experiments

1-D $^1$H NMR spectra in $H_2O/D_2O$ 90/10 v/v were recorded with a gradient-based *zgesgp* pulse sequence and solvent suppression with 1D excitation sculpting using 180 water-selective pulses, 1.7 s acquisition time, 10.55 μs 90° excitation pulses (p1), 1 s relaxation delay (d1), 2048 scans, 32k total data point and 0.3 Hz exponential line broadening.

Phase sensitive 2D $^1$H-$^1$H double quantum filter correlation spectroscopy (DQF-COSY) with gradient *cosydfesgpph* pulses and solvent suppression using 1D excitation sculpting were recorded using acquisition times of 0.1420 s in F2 and 0.0355 s in F1, 10.62 μs 90° excitation pulses (p1), 2 s relaxation delay (d1), 32 scans/512 experiments, 2k total data

point and F1 States-TPPI acquisition mode. The spectrum was computed to a 2048×1024 matrix with 1Hz (F2) and 0.3 Hz (F1) exponential multiplication and squared shifted sine bell in both dimensions (Π/9).

Total correlation spectroscopy (TOCSY) (*dipsi2esgpph*) with homonuclear Hartman-Hahn transfer using mixing sequence DIPSI-2 (decoupling in presence of scalar interaction, *dipsi2ph*), water suppression, excitation sculpting with gradients (ES element) and F1 States-TPPI States-Haberkorn-Ruben method-time proportional phase incrementation) acquisition mode for indirect detection was recorded with acquisition times of 0.1310 s in F2 and 0.0327 s in F1, 10.65 μs 90° excitation pulses (p1), 1.5 s relaxation delay (d1), 60 ms mixing time (d9), 32 scans in F1 over 512 experiments in F2, spectral width of 7812 Hz (13.01 ppm), frequency offset of 2820 Hz (4.7 ppm) and 2k total data point. The spectrum was computed to a 2048×1024 matrix with 1Hz (F2) and 0.3 Hz (F1) exponential multiplication and squared shifted sine bell in both dimensions (Π/2).

2D nuclear Overhauser effect spectroscopy correlation (NOESY) with water suppression using excitation sculpting with *noesyesgpph* gradients was recorded with acquisition times of 0.1310 s in F2 and 0.0328 s in F1, 7 μs 90° excitation pulses (p1), 1.5 s relaxation delay (d1), 300 ms mixing time (d8), 32 scans in F2 over 512 experiments in F1, spectral width (SW) 7812 Hz (13.02 ppm), frequency offset (O1) 2821 Hz (O1P 4.7 ppm) and 2k total data point. Spectrum was computed to a 2048×1024 matrix with 1Hz (F2) and 0.3 Hz (F1) exponential multiplication and squared shifted sine bell in both dimensions (Π/2).

Toner powder (~8 mg) was dissolved in 600 μL $CDCl_3$ (99.95% 2H) containing 0.1 % v/v of trimethylsilane as internal standard (Aldrich, Steinheim, Germany). The solubility of toner powder in $D_2O$ was extremely limited, making $^{13}C$ detection impractical. The change in the chemical shift can be accurately assessed following a previously published method (55). 1-D $^{1}H$-NMR spectra of toner powder in $CDCl_3$ were recorded with the conventional *zg30* pulse sequence, 2.32 s acquisition time, 8 μs 90° excitation pulses (p1), 1 ms relaxation delay (d1), 512 scans, total data point 65K (TD), 0.3 Hz exponential line broadening.

Magnitude-mode gradient-enhanced ge-2D COSY were recorded using *cosygpppqf* gradient pulses for selection and using purge pulses before d1, using acquisition times of 0.1638 s in F2 and 0.0102 s in F1, 7 μs 90° excitation pulses (p1), 2 s relaxation delay (d1), 128 scans/128 experiments and Total Data point 2K (TD). Single phase detection QF (quadrature off) was used for F1 indirect detection. Spectrum was computed to a 2048×1024 matrix with 1Hz (F2) and 0.3 Hz (F1) exponential multiplication and squared shifted sine bell in both dimensions (Π/9).

Phase-cycled TOCSY with homonuclear Hartman-Hahn transfer using mixing sequence DISPSI-2 and F1 States-TPPI (States-Haberkorn-Ruben method-Time proportional phase incrementation) acquisition mode was recorded with acquisition times of 0.1420 s in F2 and 0.0177 s in F1, 5.22 μs 90° excitation pulses (p1), 2s relaxation delay (d1), 80 ms mixing time (d9), 64 scans over 256 experiments, spectral width of 7211 Hz and 2k total data points. The spectrum was computed to a 2048×1024 matrix with 1Hz (F2) and 0.3 Hz (F1) exponential multiplication and squared shifted sine bell in both dimensions (Π/2).

NOESY spectra were obtained with *noesygpph* gradient pulses during mixing time with acquisition times of 0.1420 s in F2 and 0.0177 s in F1, 7.24 μs 90° excitation pulses (p1), 2 s relaxation delay (d1), 300 ms mixing time (d8), 64 scans in F2 over 256 experiments in F1, spectral width of 7812 Hz (13.02 ppm), frequency offset (O1) 2821 Hz (O1P 4.7 ppm), 2k total data point and F1 TPPI acquisition mode. The spectrum was computed to a 2048×1024 matrix with 1Hz (F2) and 0.3 Hz (F1) exponential multiplication and squared shifted sine bell in both dimensions (Π/2).

### 2D $^{1}$H-$^{13}$C experiments

2D Heteronuclear $^{1}$H-$^{13}$C correlation spectra of toner powder and PEPs in $CDCl_3$ and $H_2O/D_2O$, respectively, were recorded using the same pulse sequences. Phase-sensitive $^{1}$H-$^{13}$C correlation via double inept transfer HSQC spectra (*hsqcetgp*) using echo-antiecho gradient selection (F1 detection mode) with decoupling during acquisition and trim pulse sequences in inept transfer were acquired under the following conditions: 64 scans in the F2 dimension over 256 experiments in the F1 dimension, 1024 data points (TD, F2), 1J CH coupling constant 145 Hz (CNST2), 16 dummy scans (DS); F2 ($^{1}$H) parameters: spectral width (SW) of 7812 Hz (13.02 ppm), frequency offset (O1) of 2821 Hz (O1P 4.7 ppm), acquisition time 65.5 ms, 7 μs (10.65 μs for PEPs samples in $H_2O/D_2O$) 90° excitation pulses (p1), 1.5 s relaxation delay (d1); F1 ($^{13}$C) parameters: SW= 24 902 Hz (165 ppm); O1 11318 Hz (75.0 ppm), acquisition time 5.1 ms, garp composite pulse 13C decoupling program (60 μs PCPD2).

$^{1}$H-$^{13}$C correlation via heteronuclear zero and double quantum coherence HMBC spectra (Heteronuclear Multiple Bond Coherence; *hmbcgplpndqf*) with low pass J-filter to suppress one-bond correlations, no decoupling during acquisition and gradient pulses for selection were acquired in the magnitude mode (QF in dimension F1) with aq = 149 (F2)/2 (F1) ms and d1 = 1.44 s, 7 μs (10.56 μs for PEPs sample in $H_2O/D_2O$) for 90° excitation pulses (p1), 128 scans in the F2 dimension over 128 experiments in the F1 dimension, 2048 data points (F2). In the F2 ($^{1}$H) dimension, spectral width (SW) was of 7812 Hz (13.02 ppm) and frequency offset (O1) was of 2821 Hz (O1P 4.7 ppm); in the F1 ($^{13}$C) dimension, SW was of 33 204 Hz (220 ppm) with O1 of 15091 Hz (100.0 ppm). HSQC and HMBC NMR spectra were computed to a 2048×1024 matrix. HSQC were computed with exponential line broadening of −20 Hz in F2 and 3 Hz in F1 and a square shifted sine bell (Π/2). HMBC spectra were computed with a normal sine bell function (SSB value set to 0). Gradient (1 ms length (p16), 200 μs recovery (d16)) enhanced sequences were used for all 2D NMR spectra.

### PAH Analysis

Pristine toner powder and the Teflon filter containing the PEPs ($PM_{0.1}$ and $PM_{2.5}$) were spiked with a deuterated PAH internal extraction standard (Acenaphthene-d10, Phenanthrene-d10, Chrysene-d12 and Perylene-d12; Ultra Scientific, North Kingston, RI, USA) and equilibrated at room temperature for 24 hours. The samples were extracted with 15 ml 1/1 (v/v) *n*-hexane/acetone by sonication in ice water for 1 hour. The extracts were loaded into a pre-conditioned StrataR SI-1 Silica (55 μm, 70 Å), 200 mg/3 mL solid phase extraction cartridge (details in SI; Phenomenex, Torrance, CA). PAHs were coeluted with 3 ml of *n*-hexane and 6 ml of methylene chloride and concentrated under a gentle stream of

nitrogen in a water bath at 35°C. All samples were analyzed on a Shimadzu QP2010S gas chromatographic - mass spectrometer equipped with a Restek Rxi-XLB capillary column (30 m × 0.25 mm i.d. × 0.25 μm film thickness). The temperature ramp was splitless injections at 280°C, oven temperature increased from 60°C to 150°C at a rate of 25°C/min (held 1 min), temperature increased to 280°C at a rate of 15°C/min (held 2 min), temperature increased to 320°C at a rate of 5°C/min and column held at 320°C for 5 min).

The identification and quantification of PAHs was done using reference standards (Ultra Scientific, North Kingston, RI, USA). Also, to further differentiate the compositional differences of toner powder and PEPs, PAHs concentration diagnostic ratios were taken into consideration. Such ratios for LMPAHs and HMPAHs are used to reconcile their presence in the atmosphere with potential emission sources (56).

### Benzo(a)pyrene (BaP) Equivalent Toxicological Concentration Estimates

Benzo(a)pyrene (BaP) equivalent (e-BaP) toxicological concentration of the PEPs, which takes into consideration TEFs of various PAHs (57), was also calculated for all samples. These factors were derived based on the relative toxicity of BaP, which has been examined most extensively in PAH toxicity studies and determined to be a probable (2A) or possible (2B) human carcinogen (58). Taking these TEFs into consideration, an e-BaP concentration can be calculated as a summation of the product of individual PAH concentrations and the respective TEFs: e-BaP concentration = Σ16(TEF × PAH concentration), where Σ16 refers to summa]on over the 16 EPA-priority PAHs. The e-BaP toxicological concentration can be defined as the concentration of BaP that is equivalent in toxicity to a mixture of PAHs assuming there are similar toxicological mechanisms for all PAHs. It must be noted that this calculation represents only the cumulative PAH contribution to toxicity based on chemical toxicology and not on nanomaterial related data that do not exist in published literature.

## Results and discussion

### Functional composition

The high-field 600-MHz $^{1}$H-NMR spectra with cryogenic detection of the toner powder, fine ($PM_{2.5}$) and ultrafine ($PM_{0.1}$) PEPs with solvent suppression showed a combination of convoluted and sharp resonances (Fig. 1). From the higher to lower magnetic fields, the spectra were composed of non-exchangeable organic hydrogen atoms attached to $sp^3$-hybridized aliphatic carbon (HCCC; $\delta_H$: 0.7 – 1.8 ppm; Fig. 1a), non-exchangeable organic hydrogen atoms attached to $sp^3$-hybridized aliphatic carbon in α-position of an allylic (HC-C=C), acetate (HC-C(=O)-O) or imino (HC-C=$NR_2$) group ($\delta_H$: 1.8 – 3.2 ppm; Fig. 1b; “allylic” analogue, thereafter), non-exchangeable organic hydrogen atoms attached to oxygenated and methoxy (HC-O; $\delta_H$: 3.3 – 4.5 ppm; Fig. 1c) groups, non-exchangeable organic hydrogen atoms attached to $sp^2$-hybridised carbon (RCH= CH-R) and anomeric protons in anhydrides (O-CH-O) ($\delta_H$: 5.0 – 6.7 ppm; Fig. 1d) and non-exchangeable organic hydrogen atoms attached to aromatic carbon (H-$C_{ar}$; $\delta_H$: 6.7 – 8.3 ppm; Fig. 1e) NMR resonances. The prevalence of convoluted resonances generated from overlapping signals with a considerable variance in abundance was higher for high-field resonances ($\delta_H$ < 3.0 ppm) in toner powder and decreased rapidly for PEPs ($PM_{2.5}$ and $PM_{0.1}$). Strong

superimposed sharp NMR resonances were indicative of the predominance of individual chemical homologues or species. The abundances of sharp resonances were more pronounced in the aliphatic section as compared to those in the oxygenated and aromatic ranges (Fig. 1).

The concentrations on the non-exchangeable organic hydrogen in the five regions are presented in Table 1. The vast majority of carbonaceous PEPs aerosol were associated with the ultrafine ($PM_{0.1}$) PEPs (54.5 mmol/g of $PM_{0.1}$ mass, 56.3 mmol/g of PEPs $PM_{2.5}$ mass). Assuming molar H/C ratios of unfunctionalized and unsaturated aliphatic (H/C=2), oxygenated aliphatics (H/C=1.1) and aromatic (H/C=0.4) (29,30), and organic carbon to organic mass conversion of 1.6 (31), the reconstructed organic mass concentration was 786.7 mg/g and 819.5 mg/g for PEPs $PM_{2.5}$ and $PM_{0.1}$, respectively. This was in agreement with previous studies showing that total OC carbon accounted for more than 90% of released PEPs (5). Similarly, the reconstructed organic mass for toner powder was 384.8 mg/g. The $sp^3$-hybridized aliphatic and “allylicanalogue” fractions accounted for 82.8%, 80.7% and 74.9% of total non-exchangeable organic hydrogen and 66.1%, 55.5% and 48.0% of reconstructed organic mass in toner powder, PEPs $PM_{2.5}$ and PEPs $PM_{0.1}$, respectively. The HC-O fraction accounted for 9.1 to 12.5% of non-exchangeable organic hydrogen and 11.5 to 17.7% of reconstructed organic mass) for toner powder, PEPs $PM_{2.5}$ and $PM_{0.1}$. The H-$C_{ar}$ fraction was enriched in PEPs $PM_{2.5}$ and $PM_{0.1}$ and represented 9.5–11.7% (as compared to 4.1% for toner powder) of the non-exchangeable organic hydrogen and 32.9–37.5% of reconstructed organic mass (as compared to 16.2% for toner powder). Olefinic non-exchangeable organic hydrogen accounted for less than 1% of the total non-exchangeable organic hydrogen concentration for both PEPs size fractions. The differences in the relative abundance of the non-exchangeable organic hydrogen (and reconstructed organic mass) of toner powder and PEPs indicated the potential modification of the molecular composition with a stronger aromatic spectral signature in PEPs as compared to that observed for toner powder.

## Structural characterization

This section describes the structural characteristics of toner powder and PEPs in qualitative terms analyzing the 1D and 2D homo-and heteronuclear NMR spectra. This results in the identification of the types of organic species that are present and their relative abundance. A limited number of resonances were assigned to specific organic compounds using reference NMR spectra. The $^1H$-$^1H$ COSY, TOCSY, NOESY, and $^1H$-$^{13}C$ HSQC and HMBC NMR spectra are presented in the Supplementary Information.

In the aliphatic region of PEPs (Fig. 1 a, b), terminal methyl ($CH_3$-), methylene (-$CH_2$-), –CH-X (X: C or O) groups have been observed with aliphatic chains within the same spin system (cf. COSY (S1)). This was further supported by the poorly resolved cross peaks in the aliphatic and aromatic regions in TOCSY, NOESY and HMBC NMR spectra (cf. TCOSY (S2), NOESY (S3) and HMBC (S5)). Resonances of $sp^3$-hybridized carbon on aromatic rings (phenyl-CH-), oxygenated group such as $HC_{sp^3}(O)$-$C_{sp^3}$-H, H-$C_{sp^3}(O)$-$C_{sp^3}(O)H$) and/or ester-derivatives (R(=O)O-$C_{sp^3}H_2$-$C_{sp^3}H(C_{sp^3}H_3)$-R(or OR)) with oxygen atoms > 2 bonds away from protons were also observed (cf. COSY (S1) and HSQC (S4)).

The NMR spectra of toner powder demonstrated convoluted peaks in the aliphatic region reflecting multiple intra-aliphatic correlations (*e.g.*, CH-$CH_x$-$C_n$H-$CH_x$-C, $n$=1,2 and x varies depending on $n$) probably due to the polymer-based chemicals in the powder and non-exchangeable organic hydrogen bonded to $sp^2$-hybridized carbon in $\alpha,\beta$-oxygenated olefins (R-$CH_2$-$C_{sp}{}^2$H=$C_{sp}{}^2$H-O-X (X: C or H)) (Fig. 1 and cf COSY (S1) and TCOSY (S2)). Overall, the prevalence of functionalized aliphatic chains declined in the order of [toner powder] > [PEPs $PM_{2.5}$] > [PEPs $PM_{0.1}$].

Tentatively identified compounds by means of authenticated spectra and reference NMR spectra included succinate ($^-$O(O=C)-$CH_{2(a)}$-$CH_{2(b)}$-(C=O)O$^-$; Su in Fig. 1; $H_a$ and $H_b$, triplet at $\delta_H$ 2.40 ppm), lactate ($CH_{3(a)}$-$CH_{(b)}$(-OH)-$COO^-$; La in Fig. 1; $H_a$, doublet at $\delta_H$ 1.35 ppm and $H_b$, multiplet at $\delta_H$ 4.20 ppm) and glycerate (HO-$CH_{2(a)}$-$CH_{(b)}$(-OH)-$COO^-$; Gla in Fig. 1; $H_a$, doublet at $\delta_H$ 1.75 ppm and $H_b$, triplet at $\delta_H$ 2.12 ppm). The abundance of these compounds also declined in the order of toner powder>PEPs $PM_{2.5}$> PEPs $PM_{0.1}$. Lastly, it was observed that the resonance of acetate ($CH_3COO$-) at $\delta_H$ 1.90 ppm was observed only in the toner powder.

Oxygenated groups (HC-O) in toner powder and PEPs (both $PM_{2.5}$ and $PM_{0.1}$) dominated by resonances attributed to oxygenated, alcohols, esters, ethers and others (with $\delta_H$ 3.8 – 4.5 ppm) and to a lesser extent by methoxy (-$OCH_3$) derivatives ($\delta_H$ 3.2 – 3.8 ppm) (Fig. 1c). The strong abundance of aliphatic alcohols, esters and ethers was further corroborated by the coupling of HC-O with $sp^3$-hybridized aliphatic carbon (cf. TCOSY (S2) and HMBC (S4)). Non-exchangeable organic hydrogen levels in alcohols, esters and ethers increased from 3.9 ± 0.1 mmol/g in toner powder to 5.2 ± 0.1 mmol/g in PEPs $PM_{2.5}$ and 6.8 ± 0.1 mmol/g in PEPs $PM_{0.1}$. Methoxy derivatives remained relatively stable (1.9 mmol/g in toner powder, and 1.5 and 2.2 mmol/g in PEPs $PM_{2.5}$ and $PM_{0.1}$, respectively). NMR resonances in the $\delta_H$ 5.4 – 5.6 ppm mostly in the toner powder and PEPs $PM_{2.5}$ is assigned to protons attached directly or in α-position to $sp^2$-hybridized olefinic carbon that is also bonded (within less than 4 bonds) to functionalized carbon ($HC_{olefin}$=$C_{olefin}$H-(C=O)-X) (cf. HSQC (S4) and HMBC (S5)). The diminishing abundance of olefinic protons in PEPs ($PM_{2.5}$ and $PM_{0.1}$) as compared to that of toner powder (Table 1) may be indicative of allylic substitution and addition of radicals including peroxy-radicals (formed from the photolysis of other organics) and free-radical polymerization. These reactions are favored by heat/light and result in the formation of functionalized organic species (32), which is known to take place during printing (2,5).

The range of aromatic protons (Fig. 1e) showed extensive variability with resonances found on toner powder and PEPs (both size fractions) and resonances found only in PEPs (predominantly in the $PM_{2.5}$ fraction, tracer quantities in $PM_{0.1}$). However, the 2-D homonuclear and heteronuclear NMR spectra were comparable indicating that organic compounds found in PEPs were structurally similar to precursors in toner powder (cf. COSY (S1) and HSQC (S5)). NMR resonances indicative of styrene-like aromatic protons are found at $\delta_H$ 7.05 ppm and 7.30 ppm caused by protons in *ortho*- and *meta*-position (H-$C_{aromatic\text{-}sp}{}^2$-$C_{aromatic\text{-}sp}{}^2$-H) (cf. COSY (S1)). The coupling of aromatic protons with $sp^3$-hybridized -$CH_2$- and terminal –$CH_3$ (cf. NOESY (S3) and HMBC (S4) within < 4 bonds indicate aliphatic chains in the *para*-position. Terephthalate was tentatively identified with a

strong single resonance at $\delta_H$ 7.97 ppm because of the magnetically equivalent protons in the aromatic ring. The $^{1}H$-$^{13}C$ NMR spectra provided couplings that are associated with terephthalate (cf. HSQC (S4) and HMBC (S5)). The resonances with $\delta_H > 8.00$ ppm found in PEPs $PM_{2.5}$ and $PM_{0.1}$ (but absent from toner powder) showed associations with styrene-like carbon and protons (cf. HSQC (S4) and HMBC (S5)). In styrene, $C_2$ and $C_6$ resonances at $\delta_C$ 113.85 ppm and $C_3$ and $C_5$ resonances at 127.53 were observed. The peak at $\delta_H$ 1.60 ppm was attributed to $CH_{2\text{-}\beta}$ of styrene and is coupled with the $C_\beta$ signal at $\delta_C$ 31.05 ppm (Fig. 2; Fig. S4). The resonance at $\delta_C$ 156.41 ppm was attributed to the $C_4$ carbon of the styrene aromatic ring. Substitution with an alkyl ether is responsible for the shift of the signal to higher field compared to $C_4$ unsubstituted resonance around 120–130 ppm.

The spectral differences between toner powder and PEPs demonstrated compositional changes leading to the accumulation of aromatic carbon with strong styrene-like molecular signature in PEPs $PM_{0.1}$. In addition, a decline in the abundance of unsaturated and oxygenated homologue was observed. These trends may be associated with the thermal decomposition of the styrene-based polymeric powder material and formation of semi-volatile heavier aromatic species, such as PAHs. Olefins and hydroxyl-like compounds are relatively reactive (compared to their saturated and carboxylic counterparts) and can be thermally oxidized or by allylic substitution lead to the formation of larger macromolecules (33). The latter pathway may be further catalyzed by the presence of highly reactive nanomaterials present in the toner powder (34). A study evaluating the emissions from photocopiers identified nalkanes (*e.g.*, tetracosane, tetracontane, octatriacontane, hexatriacontane) in both the toner (10 to 2670 ppm) and in all sampled airborne fractions (2 to 10 ng/$m^3$) (1).

To determine the effect of the temperature on toner powder composition, specimens of toner powder were thermally-treated at 100°C, 150°C and 200°C for 5-min under atmospheric pressure. Under typical operating conditions in laser printers, temperatures up to 200°C may be developed to permanently attach the polymeric toner powder to the paper (*i.e.*, fusion). Figure 2 shows the functional composition of thermally-treated toner powder. The $^{1}H$-NMR spectra of toner powder for the five treatments are presented in Figure S6. For all thermally-treated toner powder, H-C was the dominant carbon type followed by $H\text{-}C_{ar}$. The relative contribution of $H\text{-}C_{ar}$ increased moderately for temperatures increasing up to 200°C and 300°C, while the percent abundance of H-C decreased. The percent abundance of aliphatic unsaturated and oxygenated remain relatively unchanged up to 200°C. These trends were indicative of possible transformation of long-aliphatic chains in the styrene-based polymeric material to aromatic carbon through pyrolytic and catalytic mechanisms related to the presence of metal/metal oxide ENPs and high-temperature process.

## PAHs

Polycyclic aromatic hydrocarbons (PAHs) have been of scientific interest due to their carcinogenic and mutagenic properties (35). It was shown here that the mean concentrations of ΣPAH increased from 7.2 ng/mg (0.00072 %) in the toner powder to 16.0 ng/mg (0.0016 %) and 67.0 ng/mg (0.0067 %) in the $PM_{0.1}$ and $PM_{2.5}$ PEPs size fractions, respectively. The individual PAH concentrations in toner powder and PEPs are presented in

Table 2, while Figure 3 shows the relative distribution patterns of PAHs in toner powder, and the $PM_{2.5}$ and $PM_{0.1}$ size fractions of PEPs. As shown, PEPs had total PAH concentrations approximately 2 to 10-fold higher than those found on toner powder. LMPAHs (two- and three- ring PAHs) including naphthalene, acenaphthylene and acenaphthene accounted for 79–96% of total PAH concentration in toner powder, while HMPAHs (pyrene, benzo[a]anthracene, chrysene, benzofluoranthenes and benzo[a]pyrene) contributed less than 5% of total PAHs. Conversely, HMPAHs (chrysene, anthracene and benzo[a]pyrene) were the most abundant components in PEPs. The concentration of four- and five-ring PAHs increased from 0.28 ng/mg in toner powder to 8.43 ng/mg (52.8% of total PAHs) and 36.32 ng/mg (54.2% of total PAHs) in PEPs $PM_{0.1}$ and $PM_{2.5}$, respectively. The HMPAHs have lower vapor pressure and, thus, have a higher tendency to be sorbed and bound to PEPs particles (36,37). Interestingly, a study characterizing the emissions from photocopiers detected PAHs in the airborne fraction at levels two to five times higher than the blank sample, but because the PAHs were not identified in the toner powder, the authors attributed the observation to possible contamination (1).

PAH concentration diagnostic ratios were also considered in the analysis to better understand the compositional differences between toner powder and PEPs. For LMPAHs, the mean [Phe/(Phe+Ant)] ratios were 0.38 for toner powder and 0.37–0.41 for PEPs, indicating relatively similar fingerprints. The mean [Fla/(Fla+Pyr)] ratio increased from 0.47 for toner powder to 0.50–0.67 for PEPs, giving this ratio the potential of being used as a method of fingerprinting PEPs. Since HMPAHs, aside from Pyrene, were not detected in toner powder, the [BaA/(BaA+Chr)] ratio was only calculated for PEPs and was found to have a mean value that ranged from 0.31 to 0.43. All diagnostic ratios were higher than those calculated for ambient PAHs released from high temperature combustion of fossil fuels (38,39), indicating that the fingerprint of PEPs using this method is unique from that of combustion processes.

The measurable change in the PAH speciation profile of the PEPs compared to that of the toner powder may be linked to the presence of ENPs, the majority of which are metals and metal oxides, on the toner. A similar finding has been reported in the incineration of nano-enabled thermoplastics that contained nanosized metal oxides (*i.e.*, titanium dioxide, iron oxide) and carbon nanotubes (28,40–42). The authors noticed not only an overall increase in the concentration of PAHs in the released lifecycle particular matter, but a distinct promotion of conversion of LMPAHs to HMPAHs compared to the pristine thermoplastic, which did not contain ENPs (28,41). This unmistakable change in chemical profile towards HMPAHs during thermal degradation of thermoplastics was concluded to be due to the presence of catalytic ENPs.

We hypothesize this same catalytic phenomenon may occur due to the additives in the toner powder, particularly because of the size and catalytic properties of the added metal/metal oxides which are also released and found in PEPs. The use of various metal/metal oxide ENPs similar to those found in toners and PEPs, such as iron, manganese, titania, zinc and copper have been known to have enhanced catalytic properties due to the increased reactivity and selectivity of these metallic particles (41,43–46). It is also worth noting that other particle formation mechanisms involving ozone, in addition to the nano scale metal and

metal oxide particles added and released form the toners during printing, have been proposed in previous studies and may also contribute to this VOC transformation phenomenon taking place and reported in this study [(1–4, 59).

Furthermore, in order to calculate potential risks for PAHs, the toxic equivalency factors (TEFs) were applied to evaluate PAHs lung cancer risk, assuming unit risk for BaP as described in the methods section. The BaP-equivalent concentrations were estimated as the product of TEFs and the concentrations for each individual PAH (Table 2). The BaP-equivalent concentrations for PEPs accounted for up to 16% of total PAHs concentration in PEPs $PM_{0.1}$ and 12% in PEPs $PM_{2.5}$. The difference between the measured and BaP-equivalent concentrations of PAHs was primarily due to variations in the concentrations of LMPAHs that did not contribute significantly to the overall carcinogenicity index, as these LMPAHs have lower carcinogenicity potential. It is worth noting that use of TEFs in estimating risks may seriously underestimate the carcinogenicity of PAHs because volatile PAHs can further react with oxidants to form highly mutagenic oxygenated and nitrated polycyclic aromatic compounds (O/N-PACs). Moreover, TEFs are based on toxicity of PAHs as a chemical and do not take into account the nanoparticle nature of the chemical compound. It is well known that, in general, the toxicity of ENPs may significantly differ from the micron-sized particles and chemicals (47–49).

While it is crucial to identify the presence of potential carcinogenic PAHs on PEPs, detailed toxicological studies establishing a mechanism of action for these PAHs is of utter importance and needed to assess potential health risks. It is worth noting that there are published studies on HMPAHs (*e.g.*, BaP) on the bioavailability and metabolism of a known comparative inhaled particle-borne carcinogen: diesel exhaust (50). The authors of that study concluded that subsequent to the inhalation of BaP-adsorbed diesel soot, the BaP quickly desorbed from the carbonaceous core and was then adsorbed, unmetabolized, into the blood stream of the exposed dogs, where it mostly underwent phase II metabolism. The findings from that study highlighted the fact that the toxicity of a particle-adsorbed BaP is mainly dictated by the ability of the PAH to be released and come in contact with the target organ/tissue. While the study only evaluated the metabolism of one PAH, it must be noted that more than 10 different PAHs were identified on the PEPs. Therefore, more toxicological studies needs to be done in order to have a clearer understanding of the impact of PAHs from PEPs on human health, particularly their reactive metabolites since they can bind to proteins and DNA and cause mutations, cancers or other adverse effects (51). Furthermore, additional analysis for other organic species beyond PAHs using GC- or LC-MS/MS for structural elucidation of other compounds would aid to better understand the complex chemistry of PEPs.

## Conclusions

The extensive analysis of organic species of PEPs described here is indicative of the synergistic effects of organics in the toners and engineered nanomaterials as shown by the marked transformation in the molecular composition of both the toner powder and PEPs during the printing process. Specifically, there is a stronger aromatic spectral signature on PEPs compared to that of the toner powder, which is suggestive of radical additions and

free-radical polymerization that are directly associated by heat and potential catalytic effects due to the presence of nanoscale metals, resulting in formation of functionalized organic species. Most importantly, such accumulation of aromatic carbons with a strong styrene-like molecular signature observed on the PEPs could possibly be associated with the formation of semi-volatile heavier aromatic species, such as PAHs. The change in PAH composition and the shift form low to high molecular weight in PEPs compared to toner powder might imply an increase the toxicity potential (*e.g.*, carcinogenic and mutagenic) of these PEPs, which raises concerns for human health implications. Considering that these nano-enabled toners are used extensively and exposures to the pollutants released by toner-based printing equipment are inevitable, in both occupational and home/office environments, a closer toxicological assessment is warranted.

## Supplementary Material

Refer to Web version on PubMed Central for supplementary material.

## Acknowledgments

The authors acknowledge funding for this study from National Institute for Occupational Safety and Health (NIOSH) and Consumer Protection Safety Commission (CPSC) (Grant # 212-2012-M-51174), National Institutes of Health (NIH) (Grant # HL007118) and National Science Foundation (CBET#1350789). The NMR experiments were performed at the UAB Cancer Center High-Field NMR Facility supported by the National Institutes of Health (NIH) (Grant # 1P30 CA-13148).

## References

1. Bello D, Martin J, Santeufemio C, Sun Q, Lee Bunker K, Shafer M, et al. Physicochemical and morphological characterisation of nanoparticles from photocopiers: implications for environmental health. Nanotoxicology [Internet]. 2013; 7(5):989–1003. Available from: http://www.tandfonline.com/doi/full/10.3109/17435390.2012.689883.
2. Pirela SV, Pyrgiotakis G, Bello D, Thomas T, Castranova V, Demokritou P. Development and characterization of an exposure platform suitable for physico-chemical, morphological and toxicological characterization of printer-emitted particles (PEPs). Inhal Toxicol [Internet]. 2014 Jun 27; 26(7):400–8. [cited 2017 May 23] Available from: http://www.tandfonline.com/doi/full/10.3109/08958378.2014.908987.
3. Lee CW, Hsu DJ. Measurements of fine and ultrafine particles formation in photocopy centers in Taiwan. Atmos Environ. 2007; 41(31):6598–609.
4. Schripp T, Wensing M, Uhde E, Salthammer T, He C, Morawska L. Evaluation of ultrafine particle emissions from laser printers using emission test chambers. Environ Sci Technol. 2008; 42(12): 4338–43. [PubMed: 18605552]
5. Pirela SV, Sotiriou GA, Bello D, Shafer M, Bunker KL, Castranova V, et al. Consumer exposures to laser printer-emitted engineered nanoparticles: A case study of life-cycle implications from nano-enabled products. Nanotoxicology [Internet]. 2015 Aug 18; 9(6):760–8. [cited 2017 May 23] Available from: http://www.tandfonline.com/doi/full/10.3109/17435390.2014.976602.
6. Martin J, Demokritou P, Woskie S, Bello D. Indoor Air Quality in Photocopy Centers, Nanoparticle Exposures at Photocopy Workstations, and the Need for Exposure Controls. Ann Occup Hyg [Internet]. 2017 Jan 1; 61(1):110–22. [cited 2017 Jun 12] Available from: https://academic.oup.com/annweh/article/61/1/110/2762739/Indoor-Air-Quality-in-Photocopy-Centers.
7. Martin J, Bello D, Bunker K, Shafer M, Christiani D, Woskie S, et al. Occupational exposure to nanoparticles at commercial photocopy centers. J Hazard Mater [Internet]. 2015; 298:351–60. Available from: http://linkinghub.elsevier.com/retrieve/pii/S0304389415004707.

8. Cohen JM, Derk R, Wang L, Godleski J, Kobzik L, Brain J, et al. Tracking translocation of industrially relevant engineered nanomaterials (ENMs) across alveolar epithelial monolayers *in vitro*. Nanotoxicology [Internet]. 2014 Aug 31; 8(sup1):216–25. [cited 2017 May 23] Available from: https://www.tandfonline.com/doi/full/10.3109/17435390.2013.879612.
9. Oberdörster G, Elder A, Rinderknecht A. Nanoparticles and the Brain: Cause for Concern? J Nanosci Nanotechnol [Internet]. 2009 Aug 1; 9(8):4996–5007. [cited 2017 May 23] Available from: http://openurl.ingenta.com/content/xref?genre=article&issn=1533-4880&volume=9&issue=8&spage=4996.
10. Sisler JD, Pirela SV, Shaffer J, Mihalchik AL, Chisholm WP, Andrew ME, et al. Toxicological Assessment of CoO and $La_2O_3$ Metal Oxide Nanoparticles in Human Small Airway Epithelial Cells. Toxicol Sci [Internet]. 2016; 150(2):418–28. Available from: https://academic.oup.com/toxsci/article-lookup/doi/10.1093/toxsci/kfw005.
11. Demokritou P, Gass S, Pyrgiotakis G, Cohen JM, Goldsmith W, McKinney W, et al. An in vivo and in vitro toxicological characterisation of realistic nanoscale $CeO_2$ inhalation exposures. Nanotoxicology [Internet]. 2013 Dec; 7(8):1338–50. [cited 2017 Jun 5] Available from: http://www.ncbi.nlm.nih.gov/pubmed/23061914.
12. Konduru NV, Murdaugh KM, Sotiriou GA, Donaghey TC, Demokritou P, Brain JD, et al. Bioavailability, distribution and clearance of tracheally-instilled and gavaged uncoated or silica-coated zinc oxide nanoparticles. Part Fibre Toxicol [Internet]. Dec 3.11(1):44. [cited 2017 Jun 5] Available from: http://particleandfibretoxicology.biomedcentral.com/articles/10.1186/s12989-014-0044-6.
13. Geiser M, Kreyling WG. Deposition and biokinetics of inhaled nanoparticles. Part Fibre Toxicol [Internet]. 2010 Jan 20.7(1):2. [cited 2017 Jun 20] Available from: http://particleandfibretoxicology.biomedcentral.com/articles/10.1186/1743-8977-7-2.
14. Pirela SV, Martin J, Bello D, Demokritou P. [cited 2017 Jun 6] Nanoparticle exposures from nano-enabled toner-based printing equipment and human health: state of science and future research needs; Crit Rev Toxicol [Internet]. 2017. May 19, 1–27. Available from: http://www.ncbi.nlm.nih.gov/pubmed/28524743%0Ahttps://www.tandfonline.com/doi/full/10.1080/10408444.2017.1318354
15. Géhin E, Ramalho O, Kirchner S. Size distribution and emission rate measurement of fine and ultrafine particle from indoor human activities. Atmos Environ. 2008; 42(35):8341–52.
16. Salthammer T, Schripp T, Uhde E, Wensing M. Aerosols generated by hardcopy devices and other electrical appliances. Environ Pollut [Internet]. 2012; 169:167–74. Available from: DOI: 10.1016/j.envpol.2012.01.028
17. Wensing M, Schripp T, Uhde E, Salthammer T. Ultra-fine particles release from hardcopy devices: Sources, real-room measurements and efficiency of filter accessories. Sci Total Environ [Internet]. 2008; 407(1):418–27. Available from: DOI: 10.1016/j.scitotenv.2008.08.018
18. Pirela SV, Miousse IR, Lu X, Castranova V, Thomas T, Qian Y, et al. Effects of Laser Printer–Emitted Engineered Nanoparticles on Cytotoxicity, Chemokine Expression, Reactive Oxygen Species, DNA Methylation, and DNA Damage: A Comprehensive in Vitro Analysis in Human Small Airway Epithelial Cells, Macrophages, and Lymphobla. Environ Health Perspect [Internet]. 2015 Jun 16; 124(2):210–9. [cited 2017 May 23] Available from: http://ehp.niehs.nih.gov/1409582.
19. Sisler JD, Pirela SV, Friend S, Farcas M, Schwegler-Berry D, Shvedova A, et al. Small airway epithelial cells exposure to printer-emitted engineered nanoparticles induces cellular effects on human microvascular endothelial cells in an alveolar-capillary co-culture model. Nanotoxicology [Internet]. 2015 Aug 18; 9(April 2016):769–79. [cited 2017 May 23] Available from: http://www.ncbi.nlm.nih.gov/pubmed/25387250.
20. Lu X, Miousse IR, Pirela SV, Melnyk S, Koturbash I, Demokritou P. Short-term exposure to engineered nanomaterials affects cellular epigenome. Nanotoxicology [Internet]. 2015; 10(2):1–11. Available from: http://www.tandfonline.com/doi/full/10.3109/17435390.2015.1025115.
21. Lu X, Miousse IR, Pirela SV, Moore JK, Melnyk S, Koturbash I, et al. *In vivo* epigenetic effects induced by engineered nanomaterials: A case study of copper oxide and laser printer-emitted engineered nanoparticles. Nanotoxicology [Internet]. 2016 May 27; 10(5):629–39. [cited 2017 May 23] Available from: http://www.tandfonline.com/doi/full/10.3109/17435390.2015.1108473.

22. Pirela SV, Lu X, Miousse I, Sisler JD, Qian Y, Guo N, et al. Effects of intratracheally instilled laser printer-emitted engineered nanoparticles in a mouse model: A case study of toxicological implications from nanomaterials released during consumer use. NanoImpact. 2016; 1:1–8. [PubMed: 26989787]
23. Khatri M, Bello D, Pal AK, Cohen JM, Woskie S, Gassert T, et al. Evaluation of cytotoxic, genotoxic and inflammatory responses of nanoparticles from photocopiers in three human cell lines. Part Fibre Toxicol [Internet]. 2013; 10(1):42. Available from: http://particleandfibretoxicology.biomedcentral.com/articles/10.1186/1743-8977-10-42.
24. Elango N, Kasi V, Vembhu B, Poornima JG. Chronic exposure to emissions from photocopiers in copy shops causes oxidative stress and systematic inflammation among photocopier operators in India. Environ Health [Internet]. 2013; 12(1):78. Available from: http://www.pubmedcentral.nih.gov/articlerender.fcgi?artid=3849716&tool=pmcentrez&rendertype=abstract.
25. Awodele O, Akindele AJ, Adebowale GO, Adeyemi OO. Polycyclic Aromatic Hydrocarbon, Haematological and Oxidative Stress Levels in Commercial Photocopier Operators in Lagos, Nigeria. Ghana Med J [Internet]. 2015 Mar; 49(1):37–43. [cited 2017 Jun 12] Available from: http://www.ncbi.nlm.nih.gov/pubmed/26339083.
26. Karimi A, Eslamizad S, Mostafaee M, Momeni Z, Ziafati F, Mohammadi S. Restrictive Pattern of Pulmonary Symptoms among Photocopy and Printing Workers: A Retrospective Cohort Study. J Res Health Sci [Internet]. 2016; 16(2):81–4. [cited 2017 Jun 12] Available from: http://www.ncbi.nlm.nih.gov/pubmed/27497775.
27. Yang C-Y, Haung Y-C. A cross-sectional study of respiratory and irritant health symptoms in photocopier workers in Taiwan. J Toxicol Environ Health A [Internet]. 2008 Aug 6; 71(19):1314–7. [cited 2017 Jun 12] Available from: http://www.ncbi.nlm.nih.gov/pubmed/18686202.
28. Singh D, Schifman LA, Watson-Wright C, Sotiriou GA, Oyanedel-Craver V, Wohlleben W, et al. Nanofiller presence enhances polycyclic aromatic hydrocarbon (PAH) profile on nanoparticles released during thermal decomposition of nano-enabled thermoplastics: Potential Environmental Health Implications. Environ Sci Technol [Internet]. 2017 May 2.51(9) [cited 2017 May 26] acs.est.6b06448. Available from: http://pubs.acs.org/doi/abs/10.1021/acs.est.6b06448.
29. Fuzzi S, Decesari S, Facchini MC, Matta E, Mircea M, Tagliavini E. A simplified model of the water soluble organic component of atmospheric aerosols. Geophys Res Lett [Internet]. 2001 Nov 1; 28(21):4079–82. [cited 2017 Jun 6] Available from: http://doi.wiley.com/10.1029/2001GL013418.
30. Chalbot MCG, Chitranshi P, Gamboa da Costa G, Pollock E, Kavouras IG. Characterization of water-soluble organic matter in urban aerosol by 1H-NMR spectroscopy. Atmos Environ [Internet]. 2016 Mar; 128(March 2016):235–45. [cited 2017 Jun 12] Available from: http://linkinghub.elsevier.com/retrieve/pii/S135223101530649X.
31. Turpin BJ, Lim H-J. Species Contributions to PM2.5 Mass Concentrations: Revisiting Common Assumptions for Estimating Organic Mass. Aerosol Sci Technol [Internet]. 2001 Jul 1; 35(1):602–10. [cited 2017 Jun 14] Available from: http://www.tandfonline.com/doi/abs/10.1080/02786820119445.
32. Hayes CJ, Merle JK, Hadad CM. [cited 2017 Jun 14] The chemistry of reactive radical intermediates in combustion and the atmosphere; Advances in Physical Organic Chemistry [Internet]. 2009. 79–134. Available from: http://linkinghub.elsevier.com/retrieve/pii/S0065316008000038
33. De Armas J, Kolis SP, Hoveyda AH. Zr-catalyzed olefin alkylations and allylic substitution reactions with electrophiles. J Am Chem Soc [Internet]. 2000 Jun; 122(25):5977–83. [cited 2017 Jun 14] Available from: http://pubs.acs.org/doi/abs/10.1021/ja000693j.
34. Alonso F, Riente P, Yus M. Transfer hydrogenation of olefins catalysed by nickel nanoparticles. Tetrahedron [Internet]. 2009; 65(51):10637–43. [cited 2017 Jun 14] Available from: http://linkinghub.elsevier.com/retrieve/pii/S0040402009015890.
35. Kim K-H, Jahan SA, Kabir E, Brown RJC. A review of airborne polycyclic aromatic hydrocarbons (PAHs) and their human health effects. Environ Int [Internet]. 2013 Oct.60:71–80. [cited 2017 Jun 20] Available from: http://linkinghub.elsevier.com/retrieve/pii/S0160412013001633.

36. Soldatova LN, Sansone S-A, Stephens SM, Shah NH. Selected papers from the 13th Annual Bio-Ontologies Special Interest Group Meeting. J Biomed Semantics [Internet]. 2011; 2(Suppl 2):I1. [cited 2017 May 30] Available from: http://jbiomedsem.biomedcentral.com/articles/10.1186/2041-1480-2-S2-I1.
37. Abdel-Shafy HI, Mansour MSM. A review on polycyclic aromatic hydrocarbons: Source, environmental impact, effect on human health and remediation. Egypt J Pet [Internet]. 2016; 25(1): 107–23. [cited 2017 May 30] Available from: http://linkinghub.elsevier.com/retrieve/pii/S1110062114200237.
38. Ravindra K, Sokhi R, Van Grieken R. Atmospheric polycyclic aromatic hydrocarbons: Source attribution, emission factors and regulation. Atmos Environ [Internet]. 2008 Apr; 42(13):2895–921. [cited 2017 May 23] Available from: http://linkinghub.elsevier.com/retrieve/pii/S1352231007011351.
39. Kasaraneni VK, Oyanedel-Craver V. Polycyclic Aromatic Hydrocarbon Contamination in Soils of San Mateo Ixtatan, Guatemala: Occurrence, Sources, and Health Risk Assessment. J Environ Qual [Internet]. 2016; 45(5):1635. [cited 2017 May 23] Available from: https://dl.sciencesocieties.org/publications/jeq/abstracts/45/5/1635.
40. Sotiriou GA, Singh D, Zhang F, Chalbot MCG, Spielman-Sun E, Hoering L, et al. Thermal decomposition of nano-enabled thermoplastics: Possible environmental health and safety implications. J Hazard Mater [Internet]. 2016 Mar.305:87–95. [cited 2017 Jun 12] Available from: http://linkinghub.elsevier.com/retrieve/pii/S0304389415302028.
41. Vejerano EP, Holder AL, Marr LC. Emissions of polycyclic aromatic hydrocarbons, polychlorinated dibenzo-p-dioxins, and dibenzofurans from incineration of nanomaterials. Environ Sci Technol [Internet]. 2013 May 7; 47(9):4866–74. [cited 2017 May 30] Available from: http://pubs.acs.org/doi/abs/10.1021/es304895z.
42. Vejerano EP, Leon EC, Holder AL, Marr LC. Characterization of particle emissions and fate of nanomaterials during incineration. Environ Sci Nano [Internet]. 2014 Jan 24; 1(2):133–43. [cited 2017 Jun 20] Available from: http://xlink.rsc.org/?DOI=C3EN00080J.
43. Du X, Zhang D, Shi L, Gao R, Zhang J. Morphology dependence of catalytic properties of Ni/CeO 2 nanostructures for carbon dioxide reforming of methane. J Phys Chem C [Internet]. 2012; 116(18):10009–16. [cited 2017 May 30] Available from: http://pubs.acs.org.ezp-prod1.hul.harvard.edu/doi/pdf/10.1021/jp300543r.
44. Cuenya BR. Synthesis and catalytic properties of metal nanoparticles: Size, shape, support, composition, and oxidation state effects. Thin Solid Films [Internet]. 2010 Apr; 518(12):3127–50. [cited 2017 Jun 6] Available from: http://linkinghub.elsevier.com/retrieve/pii/S004060901000057X.
45. Beletskaya IP, Cheprakov AV. Copper in cross-coupling reactions: The post-Ullmann chemistry. Coord Chem Rev [Internet]. 2004 Dec; 248(21–24):2337–64. [cited 2017 Jun 6] Available from: http://linkinghub.elsevier.com/retrieve/pii/S0010854504002383.
46. Chen T, Rodionov VO. Controllable Catalysis with Nanoparticles: Bimetallic Alloy Systems and Surface Adsorbates. ACS Catal [Internet]. 2016; 6(6):4025–33. [cited 2017 Jun 6] Available from: http://pubs.acs.org.ezp-prod1.hul.harvard.edu/doi/pdf/10.1021/acscatal.6b00714.
47. Choi J, Zhang Q, Reipa V, Wang NS, Stratmeyer ME, Hitchins VM, et al. Comparison of cytotoxic and inflammatory responses of photoluminescent silicon nanoparticles with silicon micron-sized particles in RAW 264.7 macrophages. J Appl Toxicol [Internet]. 2009 Jan; 29(1):52–60. [cited 2017 Jun 14] Available from: http://doi.wiley.com/10.1002/jat.1382.
48. Sahu D, Kannan GM, Tailang M, Vijayaraghavan R. *In Vitro* Cytotoxicity of Nanoparticles: A Comparison between Particle Size and Cell Type. J Nanosci [Internet]. 2016 Aug 23.2016:1–9. [cited 2017 Jun 14] Available from: http://www.hindawi.com/journals/jns/2016/4023852/.
49. Richter A, Sadowski J. Central European Journal of Physics. Vol. 5. Wiley; 2011. Nanoscience and nanotechnology [Internet]; 2010–2011. Available from: http://www.springerlink.com/index/X51K18326183J172.pdf [cited 2017 Jun 14]
50. Gerde P, Muggenburg Ba, Lundborg M, Dahl aR. The rapid alveolar absorption of diesel soot-adsorbed benzo[a]pyrene: bioavailability, metabolism and dosimetry of an inhaled particle-borne carcinogen. Carcinogenesis [Internet]. 2001 May 1; 22(5):741–9. [cited 2017 Jun 20] Available from: https://academic.oup.com/carcin/article-lookup/doi/10.1093/carcin/22.5.741.

51. Armstrong B, Hutchinson E, Unwin J, Fletcher T. Lung cancer risk after exposure to polycyclic aromatic hydrocarbons: A review and meta-analysis. Environ Health Perspect [Internet]. 2004 Jun; 112(9):970–8. [cited 2017 Jun 20] Available from: http://www.ncbi.nlm.nih.gov/pubmed/15198916.
52. Demokritou P, Lee SJ, Ferguson ST, Koutrakis P. A compact multistage (cascade) impactor for the characterization of atmospheric' aerosols. J Aerosol Sci [Internet]. 2004 Mar; 35(3):281–99. [cited 2017 Jun 23] Available from: http://linkinghub.elsevier.com/retrieve/pii/S0021850203004361.
53. Pal AK, Watson CY, Pirela SV, Singh D, Chalbot MCG, Kavouras I, et al. Linking exposures of particles released from nano-enabled products to toxicology: An integrated methodology for particle sampling, extraction, dispersion, and dosing. Toxicol Sci [Internet]. 2015 Aug; 146(2): 321–33. [cited 2017 May 23] Available from: https://academic.oup.com/toxsci/articlelookup/doi/10.1093/toxsci/kfv095.
54. Demokritou P, Kavouras IG, Ferguson ST, Koutrakis P. Development of a High Volume Cascade Impactor for Toxicological and Chemical Characterization Studies. Aerosol Sci Technol [Internet]. 2002 Sep; 36(9):925–33. [cited 2017 Jun 6] Available from: http://www.tandfonline.com/doi/abs/10.1080/02786820290092113.
55. Fulmer GR, Miller AJM, Sherden NH, Gottlieb HE, Nudelman A, Stoltz BM, et al. NMR chemical shifts of trace impurities: Common laboratory solvents, organics, and gases in deuterated solvents relevant to the organometallic chemist. Organometallics [Internet]. 2010 May 10; 29(9):2176–9. [cited 2017 Jun 14] Available from: http://pubs.acs.org/doi/abs/10.1021/om100106e.
56. Schifman LA, Boving TB. Spatial and seasonal atmospheric PAH deposition patterns and sources in Rhode Island. Atmos Environ [Internet]. 2015 Nov.120:253–61. [cited 2017 May 23] Available from: http://linkinghub.elsevier.com/retrieve/pii/S1352231015303010.
57. Nisbet ICT, LaGoy PK. Toxic equivalency factors (TEFs) for polycyclic aromatic hydrocarbons (PAHs). Regul Toxicol Pharmacol [Internet]. 1992 Dec; 16(3):290–300. [cited 2017 May 23] Available from: http://www.ncbi.nlm.nih.gov/pubmed/1293646.
58. Yu H. Environmental Carcinogenic Polycyclic Aromatic Hydrocarbons: Photochemistry and Phototoxicity. J Environ Sci Heal Part C [Internet]. 2002 Nov; 20(2):149–83. [cited 2017 Jun 12] Available from: http://www.tandfonline.com/doi/abs/10.1081/GNC-120016203.
59. Kowalska J, Szewczyńska MG, Pośniak M. Measurements of chlorinated volatile organic compounds emitted from office printers and photocopiers. Environ Sci Pollut Res. 2015; 22:5241–5252. (2014).

## Environmental Significance Statement

It has been shown that toners used in various printing equipment contain engineered nanomaterials (ENMs), which become airborne during printing. Toxicological evidence continues to grow confirming bioactivity of such Printer-Emitted Particles (PEPs). A major knowledge gap in risk assessment of such exposures is the characterization of complex organic chemistry of PEPs. The extensive analysis of organic species of PEPs described here indicates synergistic effects of organics in the toners and ENMs as shown by the marked transformation in molecular composition of PEPs. The observed change in PAH composition and the shift from low to high molecular weight in PEPs compared to toner powder would increase the toxicity potential (*e.g.*, carcinogenic, mutagenic) of PEPs, raising concerns for human health implications.

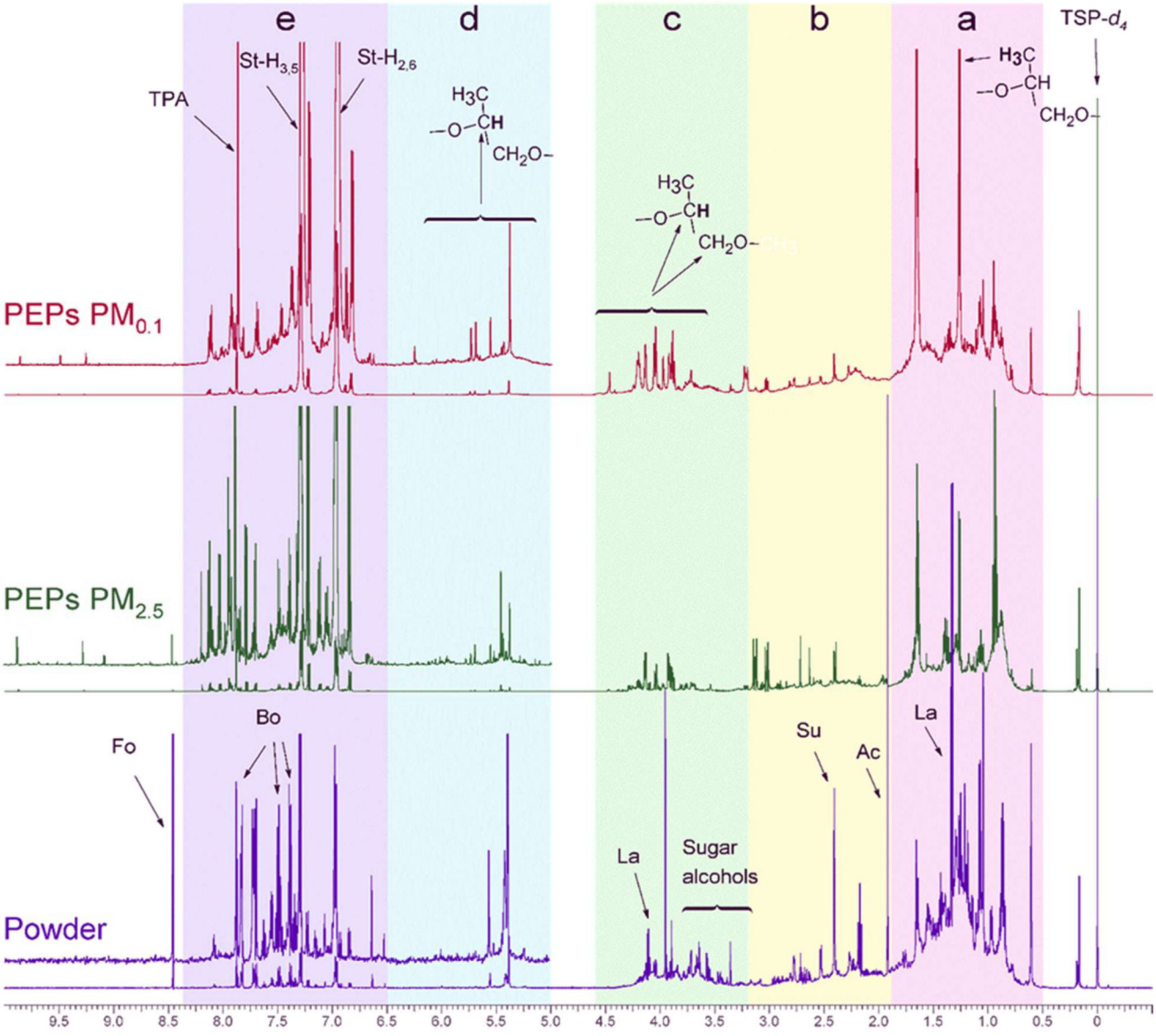


**Figure 1.**

1H NMR spectra ($\delta_H$ 0 – 10.5 ppm) of toner powder, $PM_{2.5}$ and $PM_{0.1}$ printer-emitted particles acquired with solvent suppression and exclusion regions for residual HDO. Functional structure are indicated from right to the left: (a) aliphatic carbon (**H**CCC); (b) "allylic-analogue" (**H**C-C=X); (c) oxygenated and methoxy (**H**C-O); (d) olefinic (R-C**H**=C**H**-R and O-C**H**-O); and (e) aromatic (**H**$C_{ar}$), The respective spectral intensities were scaled to 100% total integral within the entire region of chemical shift ($\delta_H$ 0.7–10.5 ppm; with residual water excluded). Fo: Formate, Bo: Benzoate, La: Lactate, Su: Succinate, Acetate:, TPA: Terephthalate.

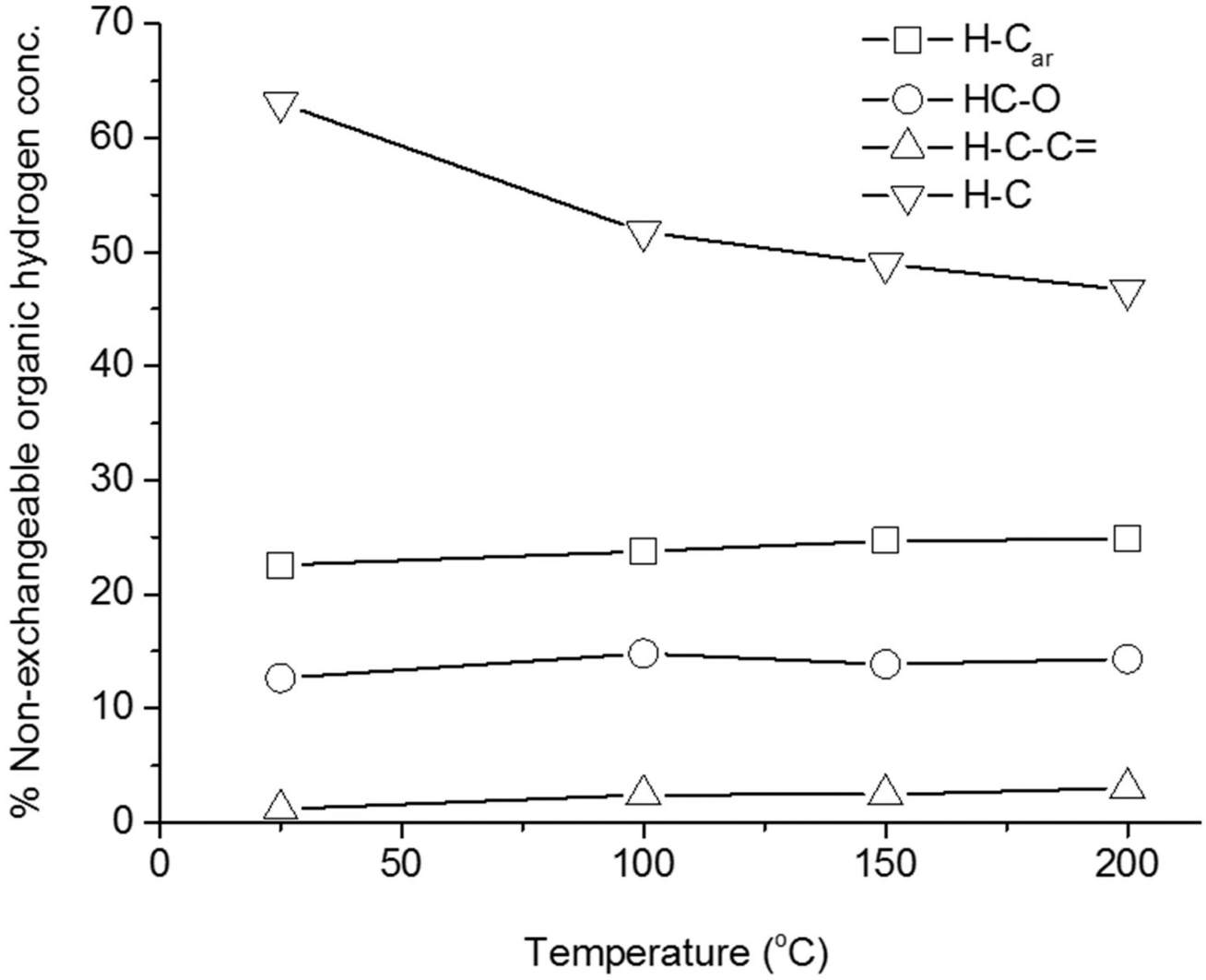


**Figure 2.**
Relative concentration pattern of H-Car, HCO, H-C-C= and H-C functional groups for thermally-treated toner powder.

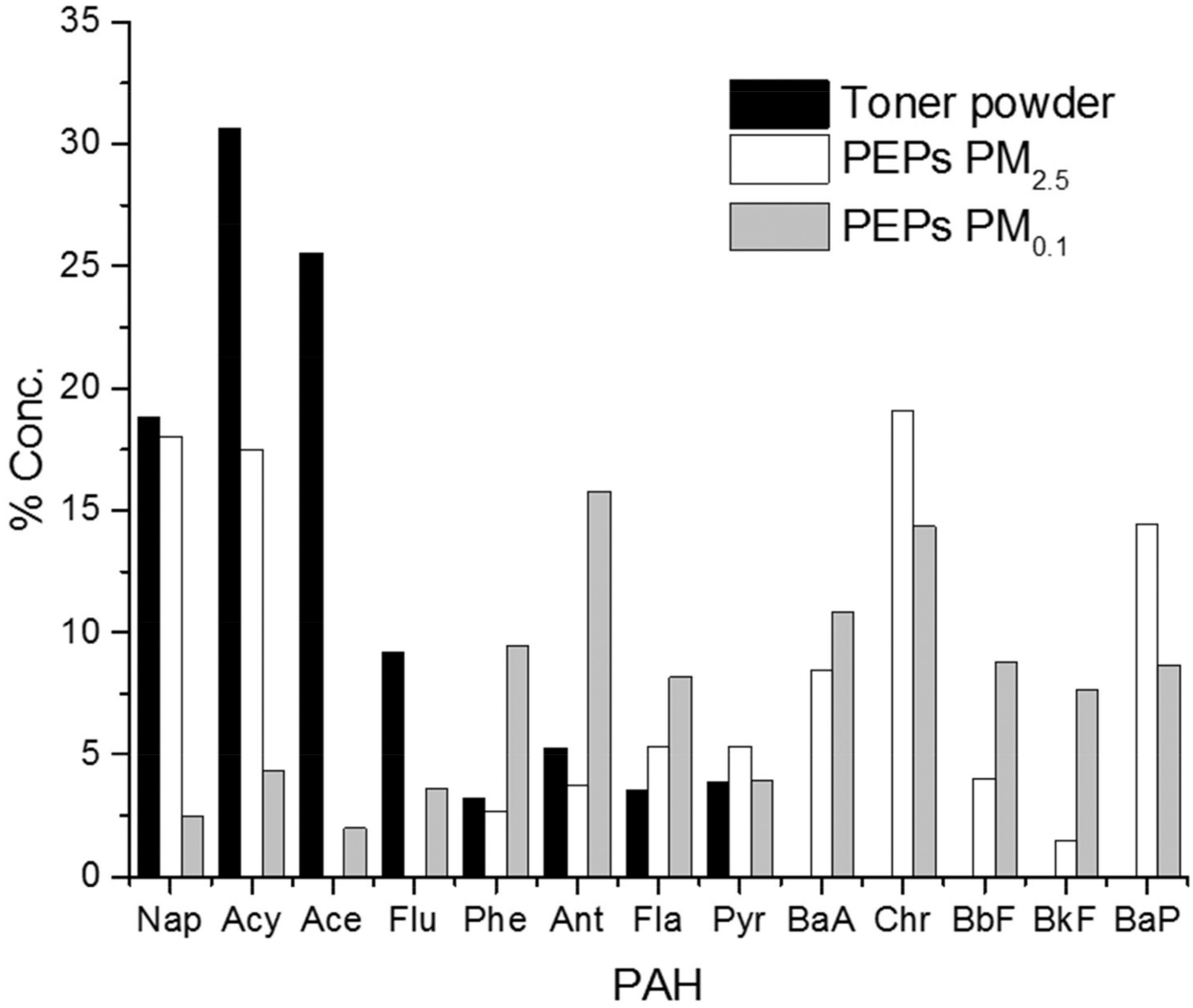


**Figure 3.**

Relative distribution of PAHs in toner powder, PEPs PM2.5 and PEPs PM0.1 (Nap: Naphthalene; Acy: Acenaphthylene; Ace: Acenaphthene; Flu:Fluorene; Phe: Phenanthrane; Ant: Anthracene; Fla: Fluoranthene; Pyr: Pyrene; BaA: Benzo[a]anthracene; Chr: Chrysene, BbF: Benzo(b/j)fluoranthene; BkF: Benzo[k]fluoranthene; BaP: Benzo[a]pyrene).

**Table 1**

Non-exchangeable organic hydrogen concentrations, in mmol/g (percent contribution in parentheses), based on 1H-NMR section integrals from printer powder and two PEPs fractions.

| | H-C | H-C-C= | H-C-O | O-CH-O & H-C= | H-$C_{ar}$ | Total |
|---|---|---|---|---|---|---|
| **Toner powder** | | | | | | |
| Conc. | 21.0 ± 0.4 | 5.5 ± 0.1 | 3.9 ± 0.1 | 0.3 ± 0.1 | 1.3 ± 0.1 | 32.0 ± 0.3 |
| % Conc. | 65.6 ± 0.2 | 17.2 ± 0.3 | 12.0 ± 0.1 | 1.1 ± 0.1 | 4.1± 0.1 | |
| **PEPs $PM_{2.5}$** | | | | | | |
| Conc. | 36.3 ± 0.2 | 9.2 ± 0.1 | 5.2 ± 0.1 | 0.3 ± 0.1 | 5.4 ± 0.1 | 56.3 ± 0.3 |
| % Conc. | 64.5 ± 0.1 | 16.2 ± 0.1 | 9.1 ± 0.1 | 0.5 ± 0.1 | 9.5 ± 0.1 | |
| **PEPs $PM_{0.1}$** | | | | | | |
| Conc. | 33.4 ± 0.3 | 7.6 ± 0.3 | 6.8 ± 0.1 | 0.2 ± 0.1 | 6.4 ± 0.1 | 54.5 ± 0.2 |
| % Conc. | 61.0 ± 0.4 | 13.9 ± 0.3 | 12.5 ± 0.1 | 0.4 ± 0.1 | 11.7 ± 0.1 | |

**Table 2**

Mean PAHs and BaP-equivalent concentrations estimated using cancer toxic equivalency factors (TEF) for individual PAHs in toner powder and PEPs $PM_{2.5}$ and PEPs $PM_{0.1}$.

| | | Concentration (ng/mg) | | | BaP equivalent concentration | | |
|---|---|---|---|---|---|---|---|
| **Compound** | **TEF** | **Toner powder** | **PEPs $PM_{0.1}$** | **PEPs $PM_{2.5}$** | **Toner powder** | **PEPs $PM_{0.1}$** | **PEPs $PM_{2.5}$** |
| Naphthalene | 0.001 | 1.3 | 2.9 | 1.7 | 0.001 | 0.003 | 0.002 |
| Acenaphthylene | 0.001 | 2.2 | 2.8 | 2.9 | 0.002 | 0.003 | 0.003 |
| Acenaphthene | 0.001 | 1.8 | 0 | 1.3 | 0.002 | 0.000 | 0.001 |
| Fluorene | 0.001 | 0.7 | 0 | 2.4 | 0.001 | 0.000 | 0.002 |
| Phenanthrene | 0.001 | 0.2 | 0.4 | 6.3 | 0.000 | 0.000 | 0.006 |
| Anthracene | 0.001 | 0.4 | 0.6 | 10.6 | 0.000 | 0.001 | 0.011 |
| Fluoranthene | 0.001 | 0.3 | 0.9 | 5.5 | 0.000 | 0.001 | 0.006 |
| Pyrene | 0.001 | 0.3 | 0.9 | 2.6 | 0.000 | 0.001 | 0.003 |
| Benzo[a]anthracene | 0.1 | 0 | 1.3 | 7.3 | 0.000 | 0.130 | 0.730 |
| Chrysene | 0.01 | 0 | 3 | 9.6 | 0.000 | 0.030 | 0.096 |
| Benzo[b/j]Fluoranthene | 0.1 | 0 | 0.6 | 5.9 | 0.000 | 0.060 | 0.590 |
| Benzo[k]Fluoranthene | 0.1 | 0 | 0.2 | 5.1 | 0.000 | 0.020 | 0.510 |
| Benzo[a]pyrene | 1 | 0 | 2.3 | 5.8 | 0.000 | 2.300 | 5.800 |
| **Total PAHs conc.** | | 7.2 | 16.0 | 67.0 | | | |
| **Total TEF-equivalent conc.** | | | | | 0.000 | 2.600 | 7.800 |
| **% TEF-equivalent/total conc.** | | | | | 0% | 16% | 12% |